

Right ventricular strain predicts functional capacity in patients with repaired tetralogy of Fallot

S. Zahra Mahshid Ojaghi Haghighi MD; Ahmad Amin MD; Feridoun Noohi MD;
Mahboobeh Daliry Fard MD; Farid Safi MD;

Hani Harati MD

Abstract

Aims-Echocardiography-derived strain rate and strain may provide new insights into right ventricular (RV) function in repaired tetralogy of Fallot (rTOF) patients in whom evaluation of RV function and functional capacity has an important role in further management.

Methods & Results-In 45 rTOF patients with severe pulmonary regurgitation, the routine echocardiography-derived indices for evaluation of RV function (TAPSE, RVOT Excursion and eyeball method) and longitudinal strain rate and strain were acquired from basal, mid and apical segments of RV free wall (RVFW) and interventricular septum; functional capacity was measured by standard Bruce protocol exercise testing. All patients had some degrees of RV dysfunction with no correlations between results of routine indices and functional capacity. Reduced RVFW average systolic strain was correlated directly with reduced functional capacity ($r = 0.86$ [$P < 0.001$]), this was also true for peak systolic strain of basal and mid segments of RVFW. Derivation of ROC curves showed that a cut-off value of 15.8% for average RVFW systolic strain predicts good exercise capacity (≥ 10 METs) with a sensitivity of 91.2% and a specificity of 100%.

Conclusions-Although routine echocardiography indices are not accurate tools in rTOF patients, systolic strain of RVFW seems to be reliable in estimation of RV function and functional capacity. (*Iranian Heart Journal 2011; 12 (3):17-36*).

Repaired Tetralogy of Fallot (rTOF) has an excellent long-term prognosis; however, survival is somewhat less than healthy people. Of all the residual lesions after rTOF,

pulmonary regurgitation (PR) is the most important hemodynamic abnormality. Arising as a sequela of right ventricular (RV) outflow dilation (a major goal of TOF correction

Received Apr. 3, 2011; Accepted for publication May. 19, 2011

Corresponding author: Ahmad Amin MD, Cardiologist, Fellowship in Heart Failure and Transplantation

Department of Heart Failure and Transplantation Rajaee Cardiovascular, Medical and Research Center, Tehran University of Medical Sciences, Vali-Asr Ave., Niyayesh Highway, Tehran, Iran. Postal Code: 199691-1151 Tel: (+98) 21 – 23922172; (+98) 912 809 8713 Fax: (+98) 21 – 22055594 Email: amina33@gmail.com

operation), pulmonary regurgitation worsens gradually and progressively deteriorates RV function, resulting in exercise intolerance, ventricular arrhythmia and death. Pulmonary valve replacement (PVR) has beneficial effects on RV size and function by eliminating the detrimental role of pulmonary regurgitation, provided it is performed early, before irreversible RV dysfunction ensues. There is still no consensus on when exactly to replace the pulmonary valve. RV function assessment should provide useful guidelines for more appropriate pulmonary valve replacement timing. Because of geometric limitations, there is no current standard for assessing RV function. Up to now, cardiac magnetic resonance imaging (CMRI) has been the most accurate method of measuring RV volume and function. Furthermore, although nuclear ventriculography (first-pass method), magnetic resonance vector mapping and three-dimensional echocardiography are well known for their better estimation of RV function, these modalities are expensive and often require proprietary systems that are not widely available.

Without any harm to the patient, echocardiography is an easily available bedside ultrasonic exam that can provide valuable data about the residual associated lesions that further impact RV function. Generating Doppler myocardial velocity measurement by echocardiography is a new method that can be used to quantify regional myocardial motion in rTOF patients and measure RV function with acceptable accuracy. RV strain rate (SR) and strain (ϵ), in which ϵ is defined as the change or deformation in distance between any two points and SR is defined as the change in velocity between these two points over the

change in length, are new and promising indices of ventricular function and are independent of geometric constraints, making them potentially useful for evaluating RV function. The present study investigates both the echocardiography-derived deformation properties (SR and ϵ) of the right ventricle in basal, mid and apical segments of the RV free wall and interventricular septum and other echocardiographic indices of RV function in rTOF patients who have severe pulmonary regurgitation. We then compare these measurements with the functional capacity of these patients. Doppler myocardial velocity measurement is a new method that has been used to quantify regional myocardial motion in RV. However, myocardial velocities detect regional motion as opposed to regional deformation. Velocities may not characterize regional function because they are composed of a combination of motions induced by segmental contraction, overall heart motion, cardiac rotation and motion induced by contraction in adjacent segments. Ultrasonic Strain Rate and Strain measurements have recently been shown to quantify local changes in myocardial deformation. Myocardial ϵ measurements have been validated in both correlative experimental sonomicrometric and clinical studies. Compared with velocities, they are less influenced by overall cardiac motion and tethering effects. Some studies have investigated the deformation properties (SR and ϵ) of the right ventricle in patients after TOF correction. Ultrasound-based ϵ measurements have been validated in experimental work with sonomicrometry and MR tagging. Moore *et al.* have presented data on longitudinal Lagrangian ϵ values for each segment of the LV derived by the MR tagging technique. Regional myocardial SR and ϵ calculations have already been shown to

quantify regional myocardial function in a variety of diseases in the LV and also for some purposes in the RV (such as RV function estimation after Senning operation)^{36, 37}

Wideman studied 33 healthy children (at University Hospital Gasthuisberg, Leuven, Belgium) without histories of cardiac disease in order to report the range of normal SR and ϵ values for both systolic and diastolic events in the LV and RV and suggested that one-dimensional ultrasound-based SR/ ϵ imaging is a sufficiently robust technique for use in clinical investigation. An advantage of ultrasound-based SR/ ϵ imaging compared with MRI is that ultrasound indices can be derived both at the bedside and (using TEE) in the operating room and ICU. They obtained 2D color Doppler myocardial imaging data for the LV and RV using standard parasternal and apical views at a high frame rate of 150 frames/second (GE Vingmed Echocardiography System V; 3.5 MHz). An interesting finding in this study was that regional ϵ values were relatively independent of resting heart rate, i.e., over the range of 65 to 120. There was also just a weak correlation of SR with either heart rate or age to the extent that they reported their values independent of heart rate or age^{36, 37}

Weidemann and his co-workers studied 30 corrected TOF patients, aged 11 ± 3 years, who had undergone surgical repair [RV outflow tract reconstruction either by a transannular patch (20 patients) or by an infundibular patch (10 patients)] at a mean age of 2 ± 1.5 years. All but three patients had at least mild postoperative pulmonary regurgitation. Patients with either residual intracardiac shunts, pulmonary stenosis with a peak systolic Doppler gradient of >20 mm Hg, elevated RV systolic pressure (tricuspid regurgitation velocity >2.5 m/s) or significant

tricuspid regurgitation were excluded from the study. All patients were asymptomatic, and no patient was taking cardiac medications. All but five patients had complete right bundle branch block (RBBB) on the electrocardiogram; all were in sinus rhythm. Ultrasound data from the TOF group were compared with 30 age-matched (10 ± 3 years; range 4 to 16) controls. Real-time, two-dimensional [editor's note: Earlier, you used "2D." Please consider using either 2D or two-dimensional exclusively.] color Doppler myocardial imaging data for longitudinal function were recorded from the RV free wall and the interventricular septum using standard apical views. Regional peak systolic velocities were significantly reduced in the basal, mid-, and apical segments of the RV free wall in patients with TOF; likewise, both longitudinal peak systolic SR and systolic ϵ were significantly reduced in the patients. In healthy children, the highest SR (-2.8 ± 0.6 second⁻¹) and ϵ ($-45 \pm 12\%$) values were found in the mid-segments. In contrast, both of these parameters were homogenous for basal (SR = -1.5 ± 0.6 second⁻¹; ϵ = $-21 \pm 8\%$), mid- (SR = -1.6 ± 0.6 second⁻¹; ϵ = $-23 \pm 9\%$), and apical (SR = -1.5 ± 0.6 second⁻¹; ϵ = $-22 \pm 7\%$) segments in TOF patients. There was no significant correlation between the longitudinal deformation parameters (SR and ϵ) measured and the degree of pulmonary regurgitation. In the septum, regional peak systolic velocities were significantly lower in basal and mid-segments, but not in apical segments, in patients with TOF compared to healthy children. In contrast, peak systolic SR (-1.4 ± 0.3 second⁻¹) and systolic ϵ ($-19 \pm 4\%$) values were homogeneously reduced in all three segments in patients with TOF. Authors [editor's question: Which authors? Please clarify.] showed that the deformation properties were reduced and homogenous within the RV

free wall when compared with age-matched healthy children in whom the highest SR and ϵ values were found in the mid-ventricular segment. The combined effects of preoperative hypertrophy and hypoxia, type of reconstruction, possible intraoperative myocardial damage and acquired postoperative lesions, such as pulmonary regurgitation, may have resulted in this impairment in RV deformation (36, 37). Solarz and co-workers studied 15 patients with corrected TOF (4 male, 11 female) and 25 control subjects (17 male, 8 female); patients with TOF were 6 ± 3 years removed from repair. All but one patient had complete RBBB [editor's note: This has already been defined.] on the electrocardiogram, and all were in sinus rhythm. They considered exclusion criteria to omit [editor's question: What do you mean by 'considered exclusion criteria to omit?' Do you mean that the authors considered having exclusion criteria to omit these effects or that the authors excluded patients with these following diseases?] the possible effect of coronary artery disease, other residual congenital problems and other systemic diseases. Ultrasound data from the TOF group were compared with 30 age-matched (10 ± 5 years; range 3 to 16) controls. The TOF group consisted of significantly more female patients who were significantly lighter and shorter than those in the control group. Although there was a trend for the TOF patients to be slightly younger, the difference was not statistically significant. Patients with TOF had little residual PS but significant residual pulmonary insufficiency and displayed an RV dimension of 2.35 ± 0.84 cm (1.4-3.4 cm) and RV thickness of 0.7 ± 0.16 cm (0.58-1.1 cm), both of which were significantly larger than that of control subjects ($P < 0.001$ for both). The RV pressure and QRS duration for patients with

TOF were 37 ± 14 mm Hg (20-60 mm Hg) and 127 ± 25 milliseconds (70-174 milliseconds), respectively. Applying 2D echocardiography, RV area was calculated from a trace of the RV in the apical four chamber view (A4) and subcostal (S) views. In the A4 view, RV length was calculated as the distance from the apex to the tricuspid annulus. In the S view, RV length was calculated from the base of the RV to the pulmonary artery valve. RV volume was then calculated by the modified ellipsoid shell model, where RV volume is equal to $2/3$ (RV area) (RV length). Authors [editor's note: Again, please clarify who you mean by 'authors.'] calculated RV volume by considering the following two formulas:

1) RV Volume $1 = 2/3$ (RV area_{A4}) (RV length_S) and

2) RV Volume $2 = 2/3$ (RV area_S) (RV length_{A4}).

RV ejection fraction (RVEF) was calculated as the difference between RV volume at end-systole and end-diastole divided by end-diastolic RV volume times 100%; therefore, two RVEF were calculated for every patient. Both RVEF1 and RVEF2 [editor's question: Do 1 and 2 refer to systole and diastole, respectively? Please clarify.] were similar for patients with TOF and control subjects ($P = 0.75$ and 0.59 , respectively) (38). For patients with postoperative TOF, systolic and diastolic SR was reduced in the RVFW, whereas these indices were similar in the IVS. ϵ was also reduced in the RVFW ($P < 0.01$) but preserved in the IVS. The authors [editor's note: Please define the authors. It is not clear if this is previous work or your own.] analyzed a more age comparable subset of control subjects. This revealed similar results (i.e., significantly diminished SR and ϵ in

the RVFW and normal SR and ϵ in the IVS). In the RVFW, reduced systolic SR and ϵ correlated with reduced RVEF ($r = -0.7$ [$P < 0.01$] and -0.6 [$P < 0.03$], respectively), and poorer early diastolic SR correlated with poorer RVEF ($r = 0.7$, $P < 0.01$). They also sought to determine if SR and ϵ abnormalities are associated with ventricular activation abnormalities as a result of RBBB (as was shown in Wideman study). Their results were not consistent with such a correlation and suggest that deformational abnormalities may be primarily because of myocardial dysfunction³⁷ The significant findings of this study are that, for patients with repaired TOF, RV dysfunction exists in the face of normal RVEF and that RVFW function is depressed; however, IVS function is preserved. These findings are significant because they suggest that RV dysfunction may be unrecognized in the absence of SR and ϵ analysis and that preserving IVS function is a potential compensatory mechanism in patients with postoperative TOF. These findings demonstrate the use of SR and ϵ indices to evaluate myocardial function because these indices can identify wall motion and contractile abnormalities in defined myocardial segments and, thus, quantify specific regions of myocardial dysfunction. In addition, these indices could possibly predict right-sided heart failure and gauge timing of PVR in repaired TOF.³⁷

Methods

1) Study group

In our case series study, 45 patients with postoperative TOF and severe pulmonary regurgitation from Rajai Heart Center (RHC), Tehran, were recruited for echocardiography and exercise stress tests (case selection lasted from August 2005 until March 2007).

Prerequisites for inclusion were a diagnosis of TOF and age range between 16 and 35 years. Participants must have had severe pulmonary regurgitation confirmed by echocardiography and also should have had only one intracardiac repair for TOF (right ventricular outflow tract reconstruction either by a transannular patch or an infundibular patch) performed more than one year before participation in the study. Patients who had previous palliative systemic-pulmonary shunt procedures (e.g., Blalock-Taussig shunt) before their complete repair were also included in this study. Exclusion criteria were: (1) age >35 years (to exclude the risk of acquired cardiovascular disease); (2) intracardiac repair within one year of the study to prevent any confounding influence related to postoperative recovery; (3) subsequent operations after the initial repair to relieve residual PS or PR (e.g., RV-PA conduit); (4) associated lesions (including VSD, ASD, aortic insufficiency, pulmonary artery or branch stenosis, PDA); (5) reduced LVEF (less than 45-50%); (6) pregnancy; (7) pacemaker; or (8) chromosomal (e.g., Down Syndrome) or other congenital anomalies. All repaired TOF patients had complete RBBB on the electrocardiogram and were in sinus rhythm. Except for one case of medically controlled rheumatoid arthritis, all patients were free of any systemic diseases.

2) Echocardiography

Echocardiography was done by Vivid 7, GE Medical Systems, with participants in a quiet, resting state. A 3 MHz frequency transducer was used to obtain routine, tissue Doppler and ϵ and SR data. Patients lay on their side in the left lateral decubitus position.

Two-dimensional, M-mode and Doppler flow echocardiography

A thorough transthoracic echocardiography (standard M mode, two-dimensional, pulsed and continuous Doppler mode) was done first to measure the following data:

- 1) RV diameter (measured at the basal third of RV in apical four chamber view);
- 2) Tricuspid regurgitation (graded according to color Doppler findings, peak tricuspid regurgitation gradient was measured by CW Doppler flow);
- 3) Pulmonary valve gradient, pulmonary regurgitation PHT (measured by CW Doppler flow in the parasternal short axis view of great vessels). The degree of pulmonary regurgitation was graded based on (I) the rate of pressure equalization between the pulmonary artery and the right ventricle assessed from pulsed Doppler traces (with PHT<100 ms assumed to represent severe pulmonary regurgitation) and (II) the width of the color jet at valve level recorded in more than one view;
- 4) Tricuspid annular plane systolic excursion (measured by M-mode at the lateral tricuspid ring in the apical four chamber view);
- 5) Right ventricle outflow tract excursion (measured by M-mode in the parasternal short axis view of great vessels); and
- 6) Global RV ejection fraction by eyeball method (measured in the apical four chamber view).

Tissue Doppler echocardiography and SR and ϵ measurements

Right ventricle peak systolic motion velocity was measured by tissue Doppler mode in apical four chamber view at lateral tricuspid ring. Right ventricular SR and ϵ were measured by echocardiography by semiautomatic frame-by-frame tissue tracking (Vivid 7, GE Medical Systems). All RV images were obtained in the apical four chamber window with a 3 MHz frequency transducer. The SR and ϵ indices were measured along the right ventricular free wall and interventricular septum at the basal (tricuspid annulus level), mid and apical segments. Because the RV geometry was frequently altered in some of these patients, the transducer sometimes had to be moved to the right to be over the RV apex or even more laterally to capture the RVFW. These measures were undertaken to ensure that the Doppler angle of insonation was zero degrees in all patients for all wall segments. Peak systolic and diastolic SR and ϵ were measured in three segments of RV free wall and three segments of IVS; in each segment, the SR and ϵ were measured for three consecutive heart beats and then averaged. Summed longitudinal RV free wall systolic strain was calculated by summing the systolic strain data of RV free wall basal, mid and apical segments. The same calculation was done for summed longitudinal RV free wall diastolic strain and summed longitudinal IVS systolic and diastolic strain. Average RV free wall systolic strain was calculated by averaging the systolic strain of base, mid and apical segments in the RV free wall.

3) Exercise stress test

All patients were scheduled for standard Bruce protocol ECG exercise stress tests to evaluate functional capacity. The patients were all in RBBB rhythm and monitored for cardiac rhythm, hemodynamic status (blood pressure and pulse) and any subjective complaint (chest pain, dyspnea, fatigue and dizziness). Patients were assessed in two groups according to their exercise capacity: those with acceptable exercise tolerance (exercise capacity equal or greater than 10 METs) and those with reduced exercise capacity (exercised less than 10 METs).

4) Statistics

Data are expressed as the mean \pm 2SD. SPSS for Windows (release 11.5.0, SPSS Inc, Chicago, Illinois) was used for basic statistical analyses. Comparisons were performed with independent sample *t*-tests. The accuracy of systolic ϵ to predict functional capacity was explored by the derivation of receiver operating characteristic (ROC) curves, which were used to designate cutoffs. An ROC curve

is a plot of the true positive rate against the false positive rate for the different possible thresholds. Here, the true positive rate is the fraction of the positive instances for which the system predicts good functional capacity (≥ 10 METs). The false positive rate is the fraction of the negative instances for which the system erroneously predicts good functional capacity. The larger the area under the curve (the more closely the curve follows the left-hand border and the top border of the ROC space), the more accurate the test will be. Probability values of $P < 0.05$ were considered statistically significant.

Results

Forty-five patients, consisting of 27 females and 18 males with mean age of 22 ± 4 years old, were included in our study. The demographic and echocardiography data can be found in Table I.

Table I. Demographic and echocardiography

<i>Demographic Data</i>			
	<i>mean</i>	<i>range</i>	<i>standard deviation</i>
<i>Age (years)</i>	22.6	18-32	4.1
<i>Height (cm)</i>	168.8	145-187	12.9
<i>Weight (kg)</i>	61.7	42-85	13.3
<i>Echocardiography Data</i>			
<i>RV diameter (cm)</i>	4.8	4.20-5.80	0.48
<i>TR peak Gradient</i>	33.2	17-57	11.16

(mmHg)			
<i>PR PHT (ms)</i>	<i>66.8</i>	<i>40-97</i>	<i>16.66</i>
<i>Echocardiography based</i>			
<i>RV function evaluation indices</i>			
<i>TAPSE (mm)</i>	<i>19.1</i>	<i>13-23</i>	<i>2.53</i>
<i>RVOT excursion (%)</i>	<i>29.5</i>	<i>12-50</i>	<i>11.33</i>
<i>SmTDI (cm/second)</i>	<i>6.5</i>	<i>5-8</i>	<i>1.12</i>

RV: Right ventricle, TR: Tricuspid regurgitation, PR: Pulmonary regurgitation, PHT: pressure half time, TAPSE: Tricuspid annular systolic excursion, RVOT: RV outflow tract, SmTDI: peak myocardial systolic velocity by tissue Doppler

Patients were found to have an *RV diameter* of 4.8 ± 1.1 cm (mean \pm 2SD), a *TR peak gradient* of 33 ± 21.4 mmHg (mostly low pressure; nine patients had TRG max of 44-57 mmHg) and a *PR PHT* of 68 ± 33 ms as measured by 2D and M-mode echocardiography. There was a direct correlation between RV end diastolic diameter and peak TR gradient ($r = 0.5$, P-value=0.003).

Routine evaluation of RV function showed an average *TAPSE* of 19.2 ± 4.8 mm, an average *RVOT excursion* of 28.57% and tissue *Doppler systolic motion velocity at lateral tricuspid ring* of 6.5 ± 2 cm/s and *IVS peak systolic motion velocity* of 5.9 ± 3.2 cm/s. By *visual (i.e., 'eyeball') methods*, 23.1%, 61.5% and 15.4% were found to have mildly, mildly to moderately and moderately reduced RV systolic function,

respectively. The tissue Doppler data also revealed a mean *E wave* of 6.33 ± 5.4 cm/s and 6.45 ± 4.4 cm/s at the lateral tricuspid ring and IVS septum, respectively and a mean of 4.5 ± 4 cm/s and 4.4 ± 3 cm/s for *A waves* at the lateral tricuspid ring and IVS septum, respectively.

There were no correlations between results of *TAPSE*, *visual method* estimation of RV function, *tissue Doppler peak systolic motion of lateral tricuspid ring* and *RVOT excursion*.

[editor's note: The use of italics throughout the text gets distracting; please reconsider using this.]

The mean values for SR and ϵ of the RV free wall and IVS segments are listed in Tables II, III and IV.

Table II. Systolic strain in segments of RV free wall and septum

<i>Systolic Strain (%)</i>	<i>Minimum</i>	<i>Maximum</i>	<i>Mean</i>	<i>Std. Deviation</i>
<i>RVFW apex</i>	<i>-7.90</i>	<i>-30.00</i>	<i>-16.4400</i>	<i>5.78892</i>
<i>RVFW mid</i>	<i>-0.80</i>	<i>-41.00</i>	<i>-22.6600</i>	<i>9.54088</i>
<i>RVFW base</i>	<i>-0.90</i>	<i>-30.00</i>	<i>-18.5378</i>	<i>7.54340</i>
<i>IVS apex</i>	<i>-28.00</i>	<i>-6.20</i>	<i>-15.8467</i>	<i>6.15115</i>
<i>IVS mid</i>	<i>-23.00</i>	<i>-2.00</i>	<i>-13.9333</i>	<i>4.81192</i>
<i>IVS base</i>	<i>-36.00</i>	<i>-9.00</i>	<i>-21.1956</i>	<i>5.91704</i>

IVS: Interventricular septum, RVFW: RV free wall

Table III.

<i>Diastolic Strain Rate (1/s)</i>	<i>Minimum</i>	<i>Maximum</i>	<i>Mean</i>	<i>Std. Deviation</i>
<i>RVFW apex</i>	<i>0.3</i>	<i>3.5</i>	<i>1.7</i>	<i>1.0136</i>
<i>RVFW mid</i>	<i>0.1</i>	<i>3.5</i>	<i>1.5</i>	<i>1.0147</i>
<i>RVFW base</i>	<i>0.3</i>	<i>4.3</i>	<i>1.8</i>	<i>1.1208</i>
<i>IVS apex</i>	<i>0.1</i>	<i>5.1</i>	<i>1.7</i>	<i>1.3789</i>
<i>IVS mid</i>	<i>0.6</i>	<i>2.7</i>	<i>1.3</i>	<i>0.6372</i>
<i>IVS base</i>	<i>0.4</i>	<i>3.5</i>	<i>1.8</i>	<i>0.8187</i>

Table IV. Diastolic strain rate in segments of RV free wall and septum

Tissue Doppler data	Exercise test METS	Mean	Std. Deviation	P-value	95% Confidence Interval of the Difference	
RVFW (Sm)	≥ 10	6.73	1.003	0.007	0.337	1.929
	< 10	5.60	1.064			
RVFW (Em)	≥ 10	7.09	2.268	0.003	1.087	4.958
	< 10	4.07	3.051			
RVFW (Am)	≥ 10	5.06	2.867	0.036	0.152	4.292
	< 10	2.83	1.750			
IVS (Sm)	≥ 10	6.03	1.803	NS	-	1.806
	< 10	5.75	0.274			
IVS (Em)	≥ 10	6.78	1.908	NS	-	3.794
	< 10	5.00	3.286			
IVS (Am)	≥ 10	4.63	1.436	NS	-	2.488
	< 10	3.50	1.643			

IVS: Interventricular septum, RVFW: RV free wall

Patients were assessed in two groups according to their exercise capacity: those with good exercise tolerance (exercise capacity equal or greater than 10 METs) and those with reduced exercise capacity (exercised less than 10 METs). Seventeen patients (37%) had reduced exercise capacity, and the rest had good capacity (63%). There was no significant difference between the *peak TR gradient* and *RV end diastolic diameter* of the two exercise capacity groups.

All patients had severe pulmonary regurgitation with *PHT* less than 100 ms. *PHT* was found to be less (indicating more severe regurgitation) in those with impaired exercise capacity (56 ± 24 ms) than those with good exercise tolerance (71

± 34 ms, P-value = 0.006); *PHT* was also correlated with exercise capacity ($r = 0.7$, P-value < 0.001).

Data analysis failed to show any significant difference between the mean value of *TAPSE* and *RVOT excursion* when comparing the good exercise capacity and the reduced exercise capacity groups. Furthermore, there was no statistically significant difference between these groups in visual method-estimated RV ejection fraction in the apical four chamber view; there was, however, a weak trend towards more reduced RV function in those with lower exercise capacity.

Tissue Doppler data analysis revealed significant differences in *RV free wall peak systolic motion velocity*, *E wave velocity* and *A wave velocity*

between the two different exercise capacity groups (P-value < 0.05, Table V).

Table V. Comparison of tissue Doppler data between functional capacity group

Systolic Strain (%)	Exercise test METS	Mean	Std. Deviation	P-Value	95% Confidence Interval of the Difference	
RVFW average	≥ 10	-21.4912	4.74541	<0.001	-12.04484	-6.59812
	< 10	-12.1697	3.43771			
RVFW apex	≥ 10	-17.2882	6.25904	NS	-7.42497	0.48486
	< 10	-13.8182	2.85721			
RVFW mid	≥ 10	-26.1471	7.29106	<0.001	-19.71626	-8.81422
	< 10	-11.8818	7.48129			
RVFW base	≥ 10	-21.0382	5.93521	<0.001	-15.14273	-5.31555
	< 10	-10.8091	6.86738			
IVS apex	≥ 10	-16.2088	7.05903	NS	-5.81033	2.84723
	< 10	-14.7273	0.46710			
IVS mid	≥ 10	-13.2647	5.07106	NS	0.02810	5.44249
	< 10	-16.0000	3.28634			
IVS base	≥ 10	-19.4647	4.96374	0.002	3.07592	11.08558
	< 10	-26.5455	5.57429			

IVS: Interventricular septum, RVFW: RV free wall

Table VI: Comparison of systolic strain in the RV free wall and septum between functional

Test Result Variable(s)	Positive if ≥	Sensitivity	Specificity
Average RVFW systolic Strain	15.8333	91.2%	100%
RVFW mid segment systolic strain	16.5000	94.1%	81.8%
RVFW basal segment systolic strain	18.5000	76.5%	81.8%

capacity groups. IVS: Interventricular septum, RVFW: RV free wall, RVFW average: average RV free wall systolic strain

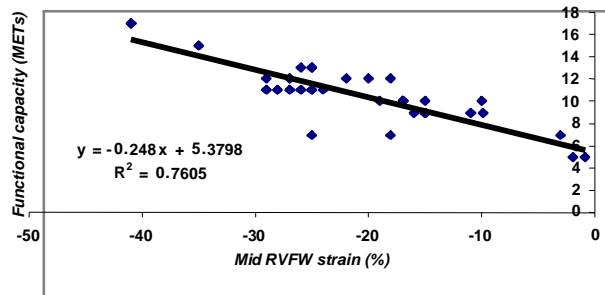
Table VIII: Average RVFW systolic strain and peak systolic strain of mid and basal segment of RV free wall cut-off points to differentiate good and poor functional capacity groups. The sensitivity and specificity values that were derived from ROC curve analysis are shown. **DVFW: RV free wall**

Echo	PHT	Normal	Total
PHT	48	33	81
Normal	3	19	22
Total	51	52	103

There was also a significant correlation between *RV free wall peak systolic motion velocity* and patients' exercise capacity ($r = 0.35$, P-value < 0.05).

Regarding the systolic strain data, there was a significant difference between the two exercise capacity groups in **peak systolic strain of basal and mid segments of RV free wall** and **basal segment of IVS** (P-value < 0.05). There were also significant correlations between exercise capacity and **peak systolic strain of basal segment of RV free wall** ($r = -0.4$, P-value = 0.01) and **peak systolic strain of basal segment of IVS** ($r = 0.58$, P-value < 0.01). A significant difference was found in the **average RV free wall systolic strain** (P-value < 0.001) between the two exercise capacity groups. This parameter was correlated significantly with exercise capacity ($r = -0.4$, P-value = 0.007). Independent t-test results are shown in Table 6, and the correlations can be found in Figs 1 to 3.

The results were used to generate ROC curves to determine the accuracy of **peak systolic strain of**



basal and mid segments of RV free wall and average RV free wall systolic strain in differentiating good and reduced exercise capacity groups.

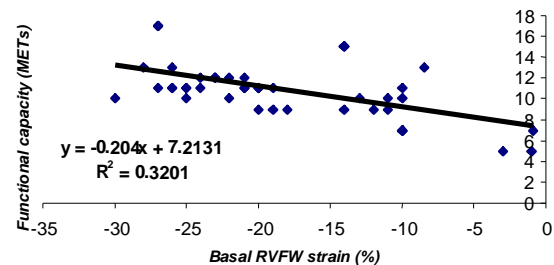


Fig.1. The correlation between systolic strain in the basal RV free wall and functional capacity

Fig.2. The correlation between systolic strain in the mid RV free wall and functional capacity

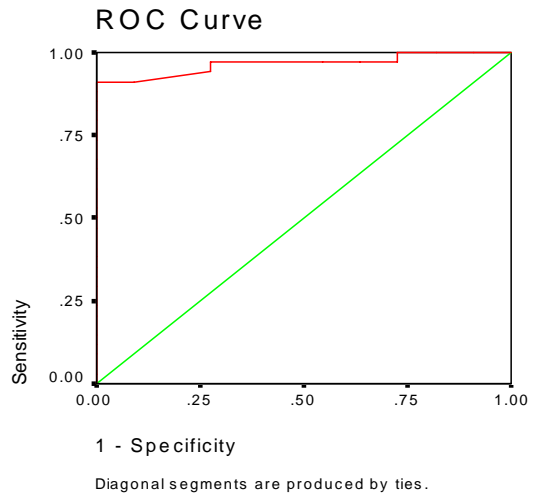
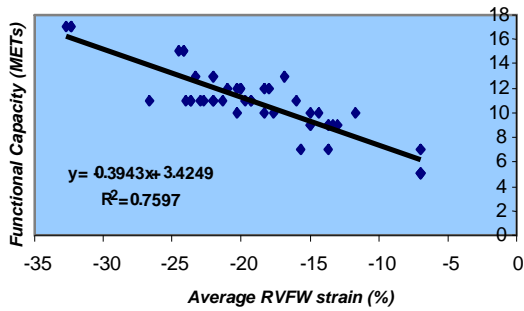
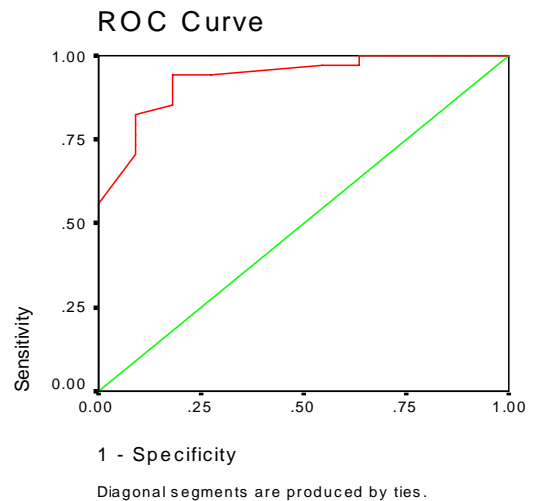
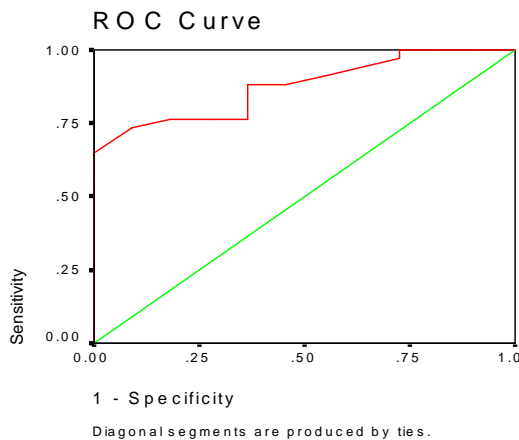


Fig.3. Correlation between average RV free wall systolic strain and functional capacity



The resultant ROC curve for **average RVFW systolic strain, peak systolic strain in the mid segment of RV free wall and peak systolic strain in the basal segment of RV free wall** had an area under the curve of **0.965, 0.932 and 0.876**, respectively, as shown in Figure 4.

Average RVFW systolic strain



Peak systolic strain in a basal RVFW segment Fig. 4: ROC curves generated to evaluate the accuracy of average RVFW systolic strain and peak systolic strain of mid and basal RV free wall segments to predict functional capacity. (Areas under curve are 0.965, 0.932, 0.876, respectively)RVFW = RV free wall

Using a cutoff value of **15.8%, average RVFW systolic strain** predicted good exercise capacity with a sensitivity of **91.2%** and a specificity of **100%**. Using a cutoff value of **16.5%, peak systolic strain of the mid segment of the RV free wall** predicted good exercise capacity with

1.

Table VIII Comparison of the systolic strain rate of interventricular septum segments between functional capacity group

Interventricular Septum Strain Rate (1/s)	Exercise test METS	Mean	Std. Deviation	P-value	95% Confidence Interval	
systolic strain rate, apical segment	>= 10	-0.924	0.7223	NS	-0.3634	1.4488
	< 10	-1.467	1.1533			
diastolic strain rate, apical segment	>= 10	1.554	0.9859	NS	-2.3240	1.2320
	< 10	2.100	2.2913			
systolic strain rate, mid segment	>= 10	-0.899	0.4457	NS	-0.1807	0.3160
	< 10	-0.967	0.2646			

a sensitivity of **94.1%** and a specificity of **81.8%**. Using a cutoff value of **18.5%, peak systolic strain of the basal segment of the RV free wall** predicted good exercise capacity with a sensitivity of **76.5%** and a specificity of **81.8%**, as depicted in Table VI..

SR data analysis revealed inconsistent results. There were significant differences between the two groups of exercise capacity in terms of peak diastolic SR at mid segment of RV free wall (P-value < 0.001), peak diastolic SR at mid segment of IVS (P-value < 0.001) and peak diastolic SR at basal segment of IVS (P-value = 0.004); however, none of these data had significant correlation with exercise capacity. There was a significant correlation between exercise capacity and peak systolic and diastolic SR at the apical segment of the RV free wall (r = -0.5, P-value = 0.1 and r = 0.7, P-value < 0.001, respectively); peak systolic SR at the basal segment of the IVS was significantly different between the two exercise capacity groups (P-value = 0.004), with a significant correlation with exercise capacity (r = 0.3, P-value = 0.4). Independent t-test results are shown in Tables VII and IX.

diastolic strain rate, mid segment	>= 10	1.464	0.6250	<0.001	0.5243	1.0037
	< 10	0.700	0.0866			
systolic strain rate, basal segment	>= 10	-1.144	0.3055	0.004	0.2805	1.0982
	< 10	-1.833	0.5220			
diastolic strain rate, basal segment	>= 10	1.905	0.7667	NS	-0.2272	1.2372
	< 10	1.400	0.9124			

Significant correlations were present between SR and ϵ values in a few segments of the RV free wall and IVS, with pulmonary regurgitation PHT

in milliseconds. Pearson correlation coefficients can be found in Tables 10, 11 and 12.

Table IX. Comparison of the systolic strain rate of RV free wall segments between functional capacity groups.

RV free wall Strain Rate (1/S)	Exercise test METS	Mean	Std. Deviation	P-value	95% Confidence Interval	
systolic strain rate, apical segment	>= 10	-1.040	0.9099	NS	-0.5196	0.2396
	< 10	-0.900	0.2598			
diastolic strain rate, apical segment	>= 10	1.950	1.0335	0.003	0.3281	1.4386
	< 10	1.067	0.5766			
systolic strain rate, mid segment	>= 10	-1.933	1.3157	NS	-1.5818	0.2491
	< 10	-1.267	1.0759			
diastolic strain rate, mid segment	>= 10	1.785	0.9793	<0.001	0.7810	1.6556
	< 10	0.567	0.3606			
systolic strain rate, basal segment	>= 10	-1.800	1.1543	NS	-0.8692	0.5359
	< 10	-1.633	0.7858			
diastolic strain rate, basal segment	>= 10	1.669	1.0677	NS	-1.4407	0.6454
	< 10	2.067	1.3029			

Table X. Pearson correlation coefficient for bivariate correlation between systolic strain and pulmonary regurgitation pressure half time; IVS: Interventricular septum, RVFW: RV free wall

<i>Systolic strain</i>	<i>IVS apex systole</i>	<i>IVS mid systole</i>	<i>IVS base systole</i>	<i>RVFW apex systole)</i>	<i>RVFW mid systole</i>	<i>RVFW base systole</i>
<i>Pearson Correlation</i>	<i>0.170</i>	<i>0.357</i>	<i>0.553</i>	<i>-0.081</i>	<i>-0.366</i>	<i>-0.013</i>
<i>P-value</i>	<i>0.322</i>	<i>0.033</i>	<i><0.001</i>	<i>0.639</i>	<i>0.028</i>	<i>0.941</i>

Table XI. Pearson correlation coefficient for bivariate correlation between systolic strain rate of septum and pulmonary regurgitation pressure half time.

<i>Strain Rate</i>	<i>IVS apex systole</i>	<i>IVS apex diastole</i>	<i>IVS mid systole</i>	<i>IVS mid diastole</i>	<i>IVS base systole</i>	<i>IVS base diastole</i>
<i>Pearson Correlation</i>	<i>0.020</i>	<i>0.028</i>	<i>-0.344</i>	<i>0.031</i>	<i>0.087</i>	<i>-0.003</i>
<i>P-value</i>	<i>0.909</i>	<i>0.873</i>	<i>0.040</i>	<i>0.856</i>	<i>0.615</i>	<i>0.987</i>

Table XII. Pearson correlation coefficient for bivariate correlation between systolic strain rate of RV free wall and pulmonary regurgitation pressure half time.

<i>Strain Rate</i>	<i>RVFW apex systole</i>	<i>RVFW apex diastole</i>	<i>RVFW mid systole</i>	<i>RVFW mid diastole</i>	<i>RVFW base systole</i>	<i>RVFW base diastole</i>
<i>Pearson Correlation</i>	<i>-0.768</i>	<i>0.753</i>	<i>-0.210</i>	<i>0.242</i>	<i>-0.037</i>	<i>-0.348</i>
<i>P-value</i>	<i><0.001</i>	<i><0.001</i>	<i>0.218</i>	<i>0.156</i>	<i>0.831</i>	<i>0.037</i>

Table XIII. Pearson correlation coefficient for bivariate correlation between interventricular septum strain rate and peak systolic motion velocity as determined by tissue Doppler.

<i>Strain Rate</i>	<i>IVS apex systole</i>	<i>IVS apex diastole</i>	<i>IVS mid systole</i>	<i>IVS mid diastole</i>	<i>IVS base systole</i>	<i>IVS base diastole</i>
<i>Pearson Correlation</i>	0.160	-0.226	-0.027	0.027	0.316	0.175
<i>P-Value</i>	0.35	0.186	0.875	0.874	0.061	0.307

Table XIV. Pearson correlation coefficient for bivariate correlation between RV free wall strain rate and peak systolic motion velocity as determined by tissue Doppler.

<i>Strain Rate</i>	<i>RVFW apex systole</i>	<i>RVFW apex diastole</i>	<i>RVFW mid systole</i>	<i>RVFW mid diastole</i>	<i>RVFW base systole</i>	<i>RVFW base diastole</i>
<i>Pearson Correlation</i>	-0.331	0.373	-0.573	0.003	0.019	-0.352
<i>P-value</i>	0.049	0.025	<0.001	0.986	0.910	0.035

Table XV. Pearson correlation coefficient for bivariate correlation between systolic strain of RV free wall and septum and peak systolic motion velocity as determined by tissue Doppler.

<i>Systolic strain</i>	<i>IVS apex systole</i>	<i>IVS mid systole</i>	<i>IVS base systole</i>	<i>RVFW apex systole)</i>	<i>RVFW mid systole</i>	<i>RVFW base systole</i>
<i>Pearson Correlation</i>	-0.049	0.275	0.208	-0.022	-0.351	-0.253
<i>P-Value</i>	0.788	0.105	0.224	0.899	0.036	0.136

Bivariate correlation analysis also showed the correlations between SR and ϵ values in some segments of the RV free wall and IVS, with RV end diastolic diameter in centimeters and peak TR gradient in mmHg. TAPSE values were correlated with peak systolic ϵ and SR of the basal segment of RV free wall but not with other SR and ϵ data. There was no correlation between RVOT excursion and either SR or ϵ data. Also, there were no correlations between the visual method of estimation of RV ejection fraction and SR and ϵ data.

Peak systolic motion velocity, as determined by tissue Doppler, correlated with most SR data of the RV free wall segment but not with other SR and ϵ data, as can be found in Tables XIII, XIV and XV.

Discussion

Cardiac morphology in Tetralogy of Fallot exposes the right ventricle to a state of pressure overload due to varying degrees of pulmonary stenosis and the unique orientation of the ventricular septal defect, which results in the right ventricular outflow tract facing the systemic great vessel. As time passes, the right ventricle compensates for this overload by increasing wall thickness, followed by increased internal diameter, but this process gradually destroys the RV myocytes and results in RV dysfunction. Other contributors to RV dysfunction are the chronic state of hypoxemia, supraventricular and ventricular arrhythmia (resulting in tachycardia cardiomyopathy) and associated lesions (resulting in RV volume overload). Total correction of tetralogy will eliminate most of these deleterious effects, but it will also bring about an inevitable hemodynamic problem (i.e., pulmonary

regurgitation) with its own deleterious effects. In the present study, we showed that all rTOF patients with severe pulmonary regurgitation consistently have dilated RV with some degrees of dysfunction. The reasons for this post-correction RV dysfunction can be addressed by two main items:

- 1) Pre-operation pressure overload, hypoxemia and associated lesions, and
- 2) Post-operation pulmonary regurgitation, tachyarrhythmia and residual associated lesions.

Relying on routine echocardiographic methods to evaluate RV function, our results showed significant derangements in interpretation of RV function as we found no consistent correlation between these methods.

Interpretation of TAPSE, one of the most popular methods of RV function evaluation, seems to be unreliable in rTOF patients, as almost all of these patients have some degree of TR. Another reason may be the presence of pulmonary regurgitation as a volume overload state with resulting exaggerated motion of the tricuspid ring in systole.

RVOT excursion is obviously impaired in these patients because the major part of the corrective surgery is to dilate the congenitally stenotic outflow tract; therefore, RVOT does not play a major role in RV pumping function. The type of reconstruction may also influence RV function. Widemen *et al.* showed that RV deformation abnormalities were more marked in patients with transannular patches versus infundibular patches.

Eyeball estimation of RV systolic function is a non-quantitative method with significant intra- and inter-observer variability. It has the advantage of considering different aspects of

RV contraction for RV function estimation, i.e., RV size, RV function relative to that of LV, RV wall thickening and endocardial excursion and deformation in different dimensions. Although still one of the most feasible and accurate methods to assess LV function, the visual method has certain limitations when estimating RV function. The very specific geometry of the RV plays a major role. Compared with the ellipsoid LV, which shortens in its longitudinal diameter mainly from apex to base, RV contraction is more complex. Estimating RV function in the apical four chamber view can at best differentiate only the extremes of spectrum of RV function; regarding repaired Tetralogy with baseline disturbances in RV function and RV dilation, the visual method is surely incapable in detecting subtle decrements in RV function, which is strongly required to define the best timing for treatment strategies (i.e., pulmonary valve replacement for pulmonary regurgitation).

Evaluating myocardial velocity by tissue Doppler imaging is a widely accepted method for RV function assessment. Measuring the peak systolic velocity of RV myocardium at the lateral tricuspid ring (Sm TDI) appears to reflect RV function in a semi-quantitative way. Our study showed a significant correlation between RV free wall peak systolic motion velocity and patients' exercise capacity. If RV dysfunction is one of the major causes of reduced exercise capacity, then Sm TDI, as an index of RV function, can predict the prognosis of an rTOF patient.

RV Strain and Strain Rate

SR and ϵ are newly introduced methods to accurately measure myocardial deformation

and offer semi-quantitative physiologic information to differentiate between normal and reduced regional RV function. These indices are free of geometric assumptions and, thus, have the potential to become the preferred reference for monitoring patients with RV dysfunction³⁸ In contrast to myocardial velocities, deformation parameters (SR and ϵ) are less influenced by tethering of myocardial segments. Jamal F *et al.* validated the use of ultrasound-derived longitudinal systolic SR and ϵ to evaluate RV function under various loading conditions. Moreover, a few clinical studies have demonstrated the benefit of myocardial velocity, SR and ϵ imaging for RV function in patients with congenital heart disease.³⁹

As RV is subjected to volume and pressure overload in many congenital heart diseases, one needs to know to what extent these parameters are influenced by different loading conditions. Experimental studies indicate that myocardial velocities and ϵ might be altered by acute changes in preload. However, the influence of preload changes on systolic velocities and SR and ϵ indices has been poorly studied in patients with congenital heart disease. Using tissue Doppler imaging, Pascotto *et al.* have shown a close correlation between RV volume overload and the regional myocardial velocities, which are clearly load-dependent. In contrast, SR and ϵ have different responses to load change. Weidemann *et al.* have shown that in normal myocardium, ϵ is influenced by acute changes in preload, follows changes in stroke volume and ejection fraction and varies with heart rate. Greenberg *et al.* showed that SR is less affected by heart rate and loading conditions and better reflects contractility. Jamal showed that acute preload reduction induces a significant decrease in RV longitudinal systolic

ϵ , whereas RV longitudinal SR does not change significantly. These observations all addressed normal myocardium.^{36, 37} Eyskens *et al.* studied the influence of preload alteration on deformation indices in patients with Atrial Septal Defect (ASD). Basically, ASD patients had greater SR and ϵ than the control patients, and there was an insignificant decrease in SR and ϵ after correcting ASD. These findings support the assumption that the RV systolic deformation properties are not significantly influenced by acute preload alterations in RV adapted myocardium and so are less load-dependent. Similar findings were reported by Abd El Rahman^{36, 37}

In our study, rTOF patients had reduced deformation indices (SR and ϵ) as compared with the normal population in both RV free wall and IVS, similar to the results of Weidemann. This suggests that the RV free wall and IVS undergo reduced contraction and relaxation as RV function deteriorates.

Considering the inclusion criteria, we believe that exercise performance in our patients reflects the contractile reserve of the right ventricle and that patients can exercise when RV dysfunction becomes more advanced. In addition, there was a direct correlation between pulmonary regurgitation PHT and exercise capacity, which implies worsened resting RV diastolic dysfunction and higher resting RV diastolic pressure in those with poor exercise tolerance.

As depicted in the Results, we found that average systolic strain of RV free wall and systolic strain in basal and mid segments of RV free wall were significantly lower in the poor exercise capacity patients. We also found a significant correlation between exercise capacity and these systolic strain values. This suggests that, despite the

complex morphology, hypertrophy, dilatation and a state of volume overload of the right ventricle, RV free wall systolic strain can be used as a reliable index to estimate functional capacity in rTOF patients. Regarding the results of ROC curve analysis, a cutoff value of 15.8% RVFW systolic strain predicted good exercise capacity with a sensitivity of 91.2% and a specificity of 100%. Although the literature has addressed SR as a load-independent index, and thus a reliable one for showing segmental contraction of myocardium, we found inconsistent results for SR. It is worthy to mention that pulmonary regurgitation causes a state of volume overload in the right ventricle, resulting in increased total right stroke volume. Therefore, we would have expected an increase in RV free wall SR. All rTOF patients have reduced systolic and diastolic SR in the segments of RV free wall, and there was no significant difference between the exercise capacity groups and no significant correlation to exercise tolerance [editor's note: This sentence is very unclear. Do you mean that there is no significant difference between exercise capacity and exercise tolerance, or do you mean "there was neither a significant difference between exercise capacities nor a significant correlation with exercise tolerance?"]. It is likely that the combination of electrical depolarization abnormalities with an increase in myocardial fibrosis are the most probable causes for the abnormal reduction in peak systolic SR in the presence of volume loading (Weidemann). Weidemann *et al.* found a significant correlation between regional deformation properties (peak systolic SR) and the QRS duration in a study on rTOF patients with pulmonary regurgitation and complete RBBB. This is consistent with the findings of the recent study by Vogel *et al.* in which they found that abnormal

depolarization (prolonged QRS duration) and repolarization (JT dispersion) were significantly associated with systolic and diastolic wall motion abnormalities. Greater QRS dispersion is characteristic of slowed interventricular conduction, leading to late electrical activation of some parts of the ventricle and paradoxical late inward motion during diastole in some regions. In particular, abnormal JT dispersion was prevalent in patients with combined systolic and diastolic wall motion abnormalities. Weidemann.^{36, 37} showed that abnormalities not only in motion, but also in deformation, are associated with an abnormally long QRS duration. The finding of mechanical-electrical interaction is in agreement with prior studies by Gatzoulis *et al.*⁴⁰ on arrhythmia and sudden cardiac death in patients with TOF. Therefore, the main cause for differences between RV free wall SR and ϵ in estimating RV function in rTOF patients may arise from the electrical abnormality (RBBB), the structural changes in RV myocardium due to fibrosis and the specific RV myocardium anatomy in these patients. Deformational indices of the interventricular septum are much more complex in rTOF patients. Some authors have shown inconsistent results. Solarz *et al.* showed preserved RV myocardial SR and systolic ϵ in the IVS, but Weidemann *et al.* revealed reduced deformational indices in septum. In our study, patients had reduced SR and ϵ in septum. An interesting finding was that peak systolic ϵ and basal diastolic and systolic SR of the mid-portion of the IVS were significantly greater in those with poor exercise tolerance; the former was inversely correlated with exercise capacity. We speculate that the IVS functions to regulate RV and LV function. This theory has been supported by previous studies that have concluded that the IVS regulates ventricular

stroke volumes to maintain proper balance between systemic and pulmonic circulation and is, thus, of critical importance to both RV and LV function. There are currently two predominant hypotheses regarding ventricular interaction: (1) series effect (i.e., because the ventricles are connected in series, the output of one ventricle must affect the output of the other), and (2) ventricular interdependence (i.e., forces from one ventricle are transmitted directly to the other). It seems logical, though speculative, that the IVS virtually compensates for the reduced function of the right ventricle in rTOF patients. Therefore, increased strain in the basal portion of IVS in more advanced RV dysfunction and poor exercise capacity is a compensation mechanism of the heart. Abnormal septal motion has been described definitively in both RV volume overload and post-operation states. Although familiar abnormality should be sought in radial deformation of the septum, abnormalities of longitudinal deformation also exist and play an important role in determining SR and ϵ of IVS. Meanwhile, the mechanical-electrical interaction regarding the high prevalence of complete RBBB in rTOF patients associated with myocardial structural changes should also influence IVS motion and deformation and add complexity to the entire issue³⁸

Conclusions

This study shows that, although routine echocardiography derived indices are not accurate to evaluate RV function in rTOF patients, systolic strain of the RV free wall can be used as a reliable tool to estimate RV function and functional capacity. This can provide useful guidelines for better timing of pulmonary valve replacement.

References

1. Davlouros P, Karatza A, Gatzoulis M, Shore D. "Timing and type of surgery for severe pulmonary regurgitation after repair of tetralogy of Fallot". *Int. J. Cardiol.* 2004; 97: 91-101.
2. Murphy JG, Gersh BJ and Mair DD. "Long-term outcome in patients undergoing surgical repair of tetralogy of Fallot." *N. Engl. J. Med.* 1993; 329: 593-599.
3. Therrien J, Marx GR and Gatzoulis MA. "Late problems in tetralogy of Fallot-recognition, management and prevention". *Cardiol. Clin.* 2002; 20: 395-404.
4. Graham Jr. TP "Management of pulmonary regurgitation after tetralogy of Fallot repair". *Curr. Cardiol. Rep.* 2002; 4: 63-67.
5. Ruzyllo W, Nihill MR, Mullins CE and McNamara DG. "Hemodynamic evaluation of 221 patients after intracardiac repair of tetralogy of Fallot". *Am. J. Cardiol.* 1974; 34: 565-576.
6. Shimazaki Y, Blackstone EH and Kirklin JW. "The natural history of isolated congenital pulmonary valve incompetence: surgical implications". *Thorac. Cardiovasc. Surg.* 1984; 32: 257-259.
7. Bove EL, Kavey RE, Byrum CJ, Sondheimer HM, Blackman MS and Thomas FD. "Improved right ventricular function following late pulmonary valve replacement for residual pulmonary insufficiency or stenosis." *J. Thorac. Cardiovasc. Surg.* 1985; 90: 50-55.
8. Ilbawi MN, Idriss FS, De Leon SY, Muster AJ, Gidding SS and Berry TMH. "Factors that exaggerate the deleterious effects of pulmonary insufficiency on the right ventricle after tetralogy repair, Surgical implications" *J. Thorac. Cardiovasc. Surg.* 1987; 93: 36-44.
9. Misbach GA, Turley K and Ebert PA. "Pulmonary valve replacement for regurgitation after repair of tetralogy of Fallot." *Ann. Thorac. Surg.* 1983; 36: 684-691.
10. Shafer RM, Foster E, Farina M, Spooner E, Sheikh F and Alley R. "Right heart reconstruction following repair of tetralogy of Fallot." *Ann. Thorac. Surg.* 1983; 35: 421-426
11. Warner KG, Anderson JE, Fulton DR, Payne DD, Geggel RL and Marx GR. "Restoration of the pulmonary valve reduces right ventricular volume overload after previous repair of tetralogy of Fallot." *Circulation.* 1993; 88(II): 189-197.
12. Wessel HU, Cunningham WJ, Paul MH, Bastanier CK, Muster AJ and Idriss FS. "Exercise performance in tetralogy of Fallot after intracardiac repair." *J. Thorac. Cardiovasc. Surg.* 1980; 80: 582-593.
13. Gatzoulis MA, Balaji S, Webber SA, Siu SC, Hokanson JS, Poile C, Rosenthal M, Nakazawa M, Moller JH, Gillette PC, Webb GD, Redington AN. "Risk factors for arrhythmia and sudden cardiac death late after repair of tetralogy of Fallot: a multicentre study." *Lancet.* 2000; 36: 975-981.
14. Strieder DJ, Aziz K, Zaver AG and Fellows KE. "Exercise tolerance after repair of tetralogy of Fallot." *Ann. Thorac. Surg.* 1975; 19: 397-405.
15. Rhodes J, Dave A, Pulling MC, Geggel RL, Marx GR and Fulton DR. "Effect of pulmonary artery stenoses on the cardiopulmonary response to exercise following repair of tetralogy of Fallot." *Am. J. Cardiol.* 1998; 81: 1217-1219.
16. Roest AAW, Helbing WA, Kunz P, Aardweg JG, Lamb HJ, Vliegen HW, Wall EE, Roos A "Exercise MR imaging in the assessment of pulmonary regurgitation and biventricular function in patients after tetralogy of fallot repair." *Radiology* 2002; 223: 204-211.
17. Kavey E, Blackman MS and Sondheimer HM. "Incidence and severity of chronic ventricular dysrhythmias after repair of tetralogy of Fallot." *Am. Heart J.* 1982; 103: 342-350.
18. Harrison DA, Harris L, Siu SC, MacLoughlin CJ, Connelly MS, Webb GD, et al. "Sustained ventricular tachycardia in adult patients late after repair of tetralogy of Fallot." *J. Am. Coll. Cardiol.* 1997; 30: 1368-1373.

19. Book WM, Parks WJ, Hopkins KL and Hurst JW. "Electrocardiographic predictors of right ventricular volume measured by magnetic resonance imaging late after total repair of tetralogy of Fallot." *Clin. Cardiol.* 1999; 22: 740–746.
20. Roos-Hesselink J, Perlroth MG, McGhie J and Spitaels S. "Atrial arrhythmias in adults after repair of tetralogy of Fallot. Correlations with clinical, exercise, and echocardiographic findings." *Circulation.* 1995; 91: 2214–2219.
21. Ebert PA. "Second operations for pulmonary stenosis or insufficiency after repair of tetralogy of Fallot." *Am. J. Cardiol.* 1982; 50: 637–640.
22. d'Udekem Y, Rubay J, Shango-Lody P, Ovaert C, Vliers A, Caliteaux M, Sluysmans T. "Late homograft valve insertion after transannular patch repair of tetralogy of Fallot." *J. Heart Valve Dis.* 1998; 7: 450–454.
23. Warner KG, Anderson JE, Fulton DR, Payne DD, Geggel RL and Marx GR. "Restoration of the pulmonary valve reduces right ventricular volume overload after previous repair of tetralogy of Fallot." *Circulation.* 1993; 88: 189–197.
24. Yemets IM, Williams WG, Webb GD, Harrison DA, McLaughlin PR, Trusler GA, Coles JG, et al. "Pulmonary valve replacement late after repair of tetralogy of Fallot." *Ann. Thorac. Surg.* 1997; 64: 526–530.
25. Eyskens B, Reybrouck T, Bogaert J, Dymarkowsky S, Daenen W, Dumoulin M, Gewillig M. "Homograft insertion for pulmonary regurgitation after repair of tetralogy of Fallot improves cardiorespiratory exercise performance." *Am. J. Cardiol.* 2000; 85: 221–225.
26. Conte S, Jashari R, Eyskens B, Gewillig M, Dumoulin M and Daenen W. "Homograft valve insertion for pulmonary regurgitation late after valveless repair of right ventricular outflow tract obstruction." *Eur. J. Cardiothorac. Surg.* 1999; 15: 143–149.
27. Ruijter FT, Weenink I, Hitchcock FJ, Meijboom EJ and Bennink GB. "Right ventricular dysfunction and pulmonary valve replacement after correction of tetralogy of Fallot." *Ann. Thorac. Surg.* 2002; 73: 1794–1800.
28. Hazekamp MG, Kurvers MMI, Schoof PH, Vliegen HW, Mulder BJM, Roest AAW, et al. "Pulmonary valve insertion late after repair of Fallot's tetralogy." *Eur. J. Cardiothorac. Surg.* 2001; 19: 667–670.
29. Vliegen HW, Straten A, Roos A, Roest AAW, Schoof PH, Zwinderman AH, et al. "Magnetic resonance imaging to assess the hemodynamic effects of pulmonary valve replacement in adults late after repair of tetralogy of Fallot." *Circulation.* 2002; 106: 1703–1707.
30. Therrien J, Siu SC, McLaughlin PR, Liu PP, Williams WG and Webb GD. "Pulmonary valve replacement in adults late after repair of tetralogy of Fallot: are we operating too late?" *J. Am. Coll. Cardiol.* 2000; 36: 1670–1675.
31. Heimdal A, D'hooge J, Bijnens B, Sutherland G, Torp H. "In vitro validation of in plane strain rate imaging, a new ultrasound technique for evaluating regional myocardial deformation based on tissue Doppler imaging." *Echocardiography* 1998; 15(8 part 2): S40.
32. Heimdal A, Stoylen A, Torp H, Skjaerpe T. "Real-time strain rate imaging of the left ventricle by ultrasound." *J Am Soc Echocardiogr* 1998 Nov; 11(11):1013-19
33. Mirsky I, Parmley WW. "Assessment of Passive Elastic stiffness for isolated heart muscle and the intact heart." *Circ Res.* 1973; 33: 233-243.
34. Lundback S. "Cardiac pumping and function of the ventricular septum." *Acta Physiol Scand Suppl* 1986; 550: 100-101
35. Carroll JD, Hess OM. "Assessment of Normal and Abnormal Cardiac Function." *Braunwald's Heart Diseases.* 2005; 1: 503-504
36. Weidemann F, Eyskens B, Mertens L, Dommke C, Kowalski M, Simmons L, et al. "Quantification of regional right and left ventricular function by ultrasonic strain rate and strain indexes after surgical repair of tetralogy of Fallot". *Am J Cardiol.* 2002; 90: 133–138.
37. Weidemann F, Eyskens B, Jamal F, Mertens L, Kowalski M, Dhooze J, et al. "Quantification of regional left and right ventricular radial and longitudinal function in healthy children using

- ultrasound-based strain rate and strain imaging". J Am Soc Echocardiogr 2002; 15: 20–28.
38. Solarz D, Witt S, Glascock BJ, Jones FD, Khoury PR, Kimball T. "Right ventricular strain rate and strain analysis in patients with repaired tetralogy of Fallot: possible interventricular septal compensation". J Am Soc Echocardiogr. 2004 Apr; 17(4):338-4
39. Kukulski JT, Strotmann J, Szilard M, D'hooge J, Bijmens B, Rademakers F, Hatle L, De Scheerder I and. Sutherland GR "Quantitation of the spectrum of changes in regional myocardial function during acute ischaemia in closed-chest pigs: An ultrasonic strain rate and strain study." J Am Soc Echocardiogr 2001; 14: 874–884

Archive of SID